

# **Facies Modelling and Reservoir Geometry of the X-Field, Niger Delta Basin, Offshore, Nigeria**

Ikomi, Misan Kelvin<sup>1</sup>, Nfor, Bruno Ndicho<sup>2</sup>

<sup>1</sup>(Department of Geology, Chukwuemeka Odumegwu Ojukwu University, Uli, Anambra State, Nigeria)

<sup>2</sup>(Department of Geology, Chukwuemeka Odumegwu Ojukwu University, Uli, Anambra State, Nigeria)

---

## **Abstract**

*Facies modelling and reservoir structural analysis was carried out using data from the X-field. Genetic units were characterized for all reservoir units from wireline logs. Based on the response of different genetic units, and the sedimentary structures displayed in the core log data, five reservoir intervals were defined (RES 01, RES 02, RES 03, RES 04, and RES 05). Results from seismic analysis suggests five exploration play facies, namely, the A facies (distal basin plain), the Bh facies (distal basin plain), the Cbh facies (reworked offshore bar/distal marine slope), the Cbl facies (distal basin plain), the D facies (proximal slope channel), and the E facies (proximal slope channel) which collectively suggests a deep-ultra marine environment. The A facies was found within the RES 03 depicting a chaotic rotated blocks, the Bh facies was identified within RES 03 and indicates high amplitude discontinuous, the Cbh facies was established in RES 02 and RES 01 and signifies high amplitude convergent, The Cbl facies was displayed in RES 03 and shows low amplitude convergent, the D facies was found in the uppermost part of the seismic section and corresponds to continuous high and low amplitude, while the E facies was found beneath the D facies in the uppermost section and corresponds to continuous low amplitude, high amplitude and Impedance. The reservoirs thinned out in the SE direction towards well 05. RES 01 and RES 02 were not correlated down to well 05 because they pinched out in well 03, thereby affecting reservoir thickness and lateral extensiveness for RES 01 and RES 02. Major faults were identified as footwall and hanging wall of same reservoir as in the case of RES 01 in well 01, Well 02, and well 03 respectively, and thick pelagic Shale was captured within the field.*

**Keyword** Facies, Modelling, Reservoir, Pelagic, Seismic

---

Date of Submission: 30-09-2021

Date of Acceptance: 14-10-2021

---

## **I. Introduction**

Facies modelling is fundamental to understanding reservoir properties (Aliakbar et al. 2016). It is a very useful approach to understand the distribution and quality of sand and shale bodies, to enhance useful fluid flow predictions. Since reservoir properties are closely related to the facies that exist within a reservoir, it is therefore necessary to carry out a facies characterization of reservoirs of the X-field alongside a structural analysis to give an understanding of reservoir architecture and geometry.

## **II. Aims and Objectives**

This study is aimed at defining the facies and their distribution within the reservoirs of the X-field and define their geometry and architecture. The specific objectives are to: define genetic units for each well, correlate sand bodies across the wells, establish structural architecture for each reservoir units, and develop reservoir attribute maps to ascertain areas of interest.

## **III. Study Area and Geology**

The area of study, X-field, is located 120km southeast of the Niger Delta Basin, and extends to about 60km<sup>2</sup> (Figure 1). It is owned by Shell Nigeria Exploration and Production Company. The Niger Delta Basin lies on the Gulf of Guinea and is between longitudes 3<sup>o</sup>E and 9<sup>o</sup>E and latitudes 4<sup>o</sup>N and 7<sup>o</sup>N (Whiteman, 1982). In accordance with the oil and gas industry confidentiality policy, the detailed location of the field was not disclosed.

The stratigraphy of the Tertiary Niger Delta is characterized of the Akata Formation, the Agbada Formation, and the Benin Formation in an ascending manner (Figure 2). At the approximate depocentre of the central part of the Niger Delta Basin, these formations are estimated to be about 28,000ft thick (Avbovo, 1978).

The Akata Formation is overlain by the Agbada Formation and is characterized by an even shale development. According to Short & Stauble (1967), these shales which are medium to dark grey, variably medium hard or soft, and partly sandy or silty are undercompacted and are likely to encompass lenses of unusually high-pressured siltstone or fine-grained sandstone.

The Agbada Formation is underlain and overlain by both the Akata Formation and the Benin Formation respectively, it is characterized by an alternation of sandstone and shale beds which were suggested by Avbovbo (1978) to be of the delta front, distributary channel and deltaic plain origin.

The Benin Formation is the topmost and is underlain by the Agbada Formation and is of a non-marine origin. It is characterized mainly by massive freshwater bearing sandstone exhibiting high porosity, and local tinny shale interbeds which are believed to be of a braided river origin. These sandstones are dominantly composed of quartz, potash feldspar and negligible quantity of plagioclase, and could signify point-bar deposits, channel fill, and natural levee while the shales may signify back swamp deposits and oxbow fills (Avbovbo, 1978; Short & Stauble, 1967).

#### **IV. Data Set and Methodology**

##### **Data Set**

This study was limited to wireline logs for five wells, 3D seismic data, and core log data for one well. The wireline log data consisted of gamma ray, neutron, density, resistivity, and sonic logs (Figure 3), which were loaded and studied with the use of Schlumberger's Petrel 2013.

##### **Facies Characterization**

The wireline log data and core data available for the X-Field was investigated, and genetic units were characterized for all reservoir units. This was done based on the responses of different genetic units to wireline logs, in conjunction with the various sedimentary structures typical of these genetic units from core log data.

##### **Correlation of Well Logs**

Using wireline log data, parasequences were correlated and loop tied through the various reservoir intervals. It was necessary to carry out a correlation study to ascertain the existence of flooding surfaces within the reservoir, since it is essential to establish the reservoir geometry.

##### **Seismic Investigation**

Five seismic horizons which were initially picked on well logs as reservoir tops were mapped across the seismic section, following reflections across the seismic volume. This was achieved by a seismic to well tie to validate horizons picked. 3D seismic lines were investigated for faults, and faults were assigned geometry according to the type of fault. These faults were displayed on the several maps developed in this study. The seismic lines were further investigated to capture exploration plays.

##### **Seismic-to-Well Tie**

The essence of seismic to well tie was to bridge the gap between seismic in time and well in depth. Well 03 was used to conduct the tie. However, Ricker 25Hz wavelet was convolved with the product of sonic and density log to generate the reflection coefficient. This was then tied to the residual seismic. Nonetheless, no time or bulk shift was done since the reservoir top tied perfectly with the peak, which invariably corresponds to the to the red which is positive (Figure 10)

##### **Seismic Attribute Maps**

Several maps were developed for the reservoir units. These were a time map, depth map, structural map, and root mean square map.

#### **V. Results and Discussion**

##### **Well Correlation**

The correlation was done in the NW-SE trending direction. It helped to identify the continuity of reservoirs within the field. Five reservoirs were identified. The reservoirs thinned out/truncated in the SE direction towards well 5. RES 01 and RES 02 were not correlated down to well 05 because they pinched out in well 03. Major faults were evident as some reservoirs were identified at both footwall and hanging wall within the field. An example is the case of RES 01 in Well 01, Well 02, and Well 03 respectively. There was a basin and range topography in the subsurface (two opposite dipping normal faults) as could be seen in well 01, well 02 and well 03, where the RES 02 in Well 01 and RES 03 is found on the footwalls while that in Well 02 is a hanging wall. Stratigraphic pinchouts were displayed by the absence of RES 01 in Well 05. Thick pelagic Shale displayed within the field (Figure 4).

### **Seismic Interpretation**

Five seismic horizons were mapped across the seismic section (Figure 11). These horizons were mapped according to the principles of stratigraphy. Several discontinuities in the reflection pattern at the mid-section of the seismic volume were observed. Horizons were picked continuously despite the displacement of reflections across the mid-section of the seismic volume. Up-warping reflections at the left section of the seismic volume was observed. Horizons terminates at the flank of the feature. Low amplitude discontinuous reflections, abrupt termination of high amplitude reflection was also observed. Horizons were mapped with ease in regions of High amplitude continuous reflections found at the uppermost part of the seismic section

Extensional and compressional tectonics related structures were picked, normal. Faults mostly trend NW-SE and dip eastwards. NE-SW trending faults also exists (Figure 12). Basin and range topography (Horst and graben). Reflectors terminating against faults. Faults acts as traps and migration pathway. Also present were NE-SW dipping regional faults.

### **Log Facies and Depositional Environment**

Analysis of the Gamma ray log indicated that the log patterns fall majorly into 3 categories using log shape patterns as defined by Cant 1992. These categories are Saw teeth (serrated) shaped, Hourglass (symmetrical) shaped, and Fine up and Sharp base (bell) shaped successions.

The bell-shaped succession is evident on well 01 at depths ranging 1600m- 1700m, well 02 at depths ranging 1650m-1720m, and well 03 at depths ranging 1700m- 1750m respectively. The saw-teeth shaped succession is evident on well 01 at depths ranging 2200m- 3800m, well 02 at depths ranging 1720m- 3000m, well 03 at depths ranging 1750m- 2700m, and well 05 at depths ranging 2000m-3400m. Also, a symmetrical shaped succession is also evident on well 01 at depth ranging from 1150m- 1600m, and 2000m-2050m (Figure 5).

The bell shaped succession is suggestive of a deep tidal channel fill, deltaic channel, proximal deep sea setting, or tidal flats. The saw-teeth shaped succession is suggestive of a deep marine slope, mixed tidal flat, or a fluvial flood plain, while the hour-glass shaped section is suggestive of a reworked offshore bar, or a regressive to transgressive shore face delta.

### **Seismic Facies and Depositional Environment**

Several kinds of exploration play facies were depicted from the seismic section considering reflection configuration after Roksandic 2006 (Figure 8) which takes into account reflection continuity, reflection amplitudes, and reflection frequencies. These seismic facies include: The A facies, the Bh facies, the Cbh facies, the Cbl facies, the D facies, the E facies. (Figure 7) The A facies corresponds to the mid-section and found within the RES03 depicting a chaotic with rotated blocks. The Bh facies was also identified in the mid-section also found within RES03 and indicates high amplitude discontinuous. The Cbh facies was seen at the upper part of the RES02 and lower part of RES01 and signifies high amplitude convergent, The Cbl facies were seen in the mid-section of the RES03 and shows low amplitude convergent. The D facies were found in the topmost part of the seismic section and corresponds to continuous high and low amplitude. While the E facies was found beneath the D facies in the uppermost section and corresponds to continuous low amplitude, high amplitude, and Impedance.

These facies are also indicative of different depositional environments. A Facies (Distal basin plain), Bh facies (Distal basin plain), Cbh facies (Reworked offshore bar/Distal deep marine slope, Cbl facies (Distal basin plain), D facies (Proximal slope channel), E facies (Proximal slope channel).

### **Structural Interpretation and Seismic Attributes**

Time and depth structural maps developed displays the major traps in the field to be a structural high situated at the south eastern flank of the field which corresponds to the roll over structure observed on the seismic section (Figure 13, 15). These structural highs in red which are the potential prospect areas and structural lows in purple are the potential source rocks.

The RMS attribute maps (Figure 17) shows clusters of bright amplitude suggesting high porosity and permeability. These bright spots are because of increased hydrocarbon saturation across the reservoir tops. Comparing the structural maps (Figure 16a-e) for each reservoir and their corresponding RMS map shows that these distinct zones of high amplitude coincide with structural highs. Therefore, a combination of reservoir structural maps and RMS attribute maps would be useful to make development decisions in the future.

## **VI. Conclusion**

This study was able to identify five reservoirs within the field. The reservoirs thinned out/truncated in the SE direction towards well 05. RES 01 and 02 were not correlated down to well 05 because they pinched out

in well 03. Some reservoirs were identified at both footwall and hanging wall within the field as in the case of RES 01 in well 01, Well 02, and well 03 respectively.

Analysis of seismic data revealed an evident basin range topography in the subsurface (two opposite dipping normal faults) as was displayed in wells 01, 02 and 03, where the RES 02 in well 01 and RES 03 is found on the footwalls while that in well 02 is a hanging wall. There was an evident regional occurrence of the thick pelagic shale within the field.

Seismic attribute maps revealed that all five reservoirs have a high degree of porosity and permeability as displayed by clusters of bright amplitude, majorly around the structural highs sited in the South eastern flank of the field.

### References

- [1]. Aliakbar B, Omid A, Abbas B, Meysam T. 2016. Facies modeling of heterogeneous carbonates reservoirs by multiple point geostatistics. *J Pet Sci Technol* 6(2): pp. 56–65
- [2]. Avbovbo AA. 1978. Tertiary lithostratigraphy of Niger Delta. *Geologic notes*. AAPG Bull 62(2): pp. 297–306
- [3]. Cant, D.J. 1992. Subsurface facies analysis. In *Facies Models: Response to Sea level Change* (Walker, R.G.; James, N.P.; editors). Geological Association of Canada, pp. 195-218
- [4]. Nton, Matthew & Esan, T.B. 2010. Sequence stratigraphy of EMI field, OFFSHORE eastern Niger Delta, Nigeria. *European Journal of Scientific Research*. 44. Pp. 115-132.
- [5]. Roksandic, M.M. 2006. Seismic facies analysis concepts. *Geophysical Prospecting*. 26. Pp. 383 - 398. 10.1111/j.1365-2478.1978.tb01600.x.
- [6]. Short KC, Stauble A. J. 1967. Outline of geology of Niger Delta. *AAPG Bull* 51(5): pp.761–779
- [7]. Whiteman A. 1982. *Nigeria: its petroleum geology, resources, and potential*, vol 1–2. Graham and Totter, London

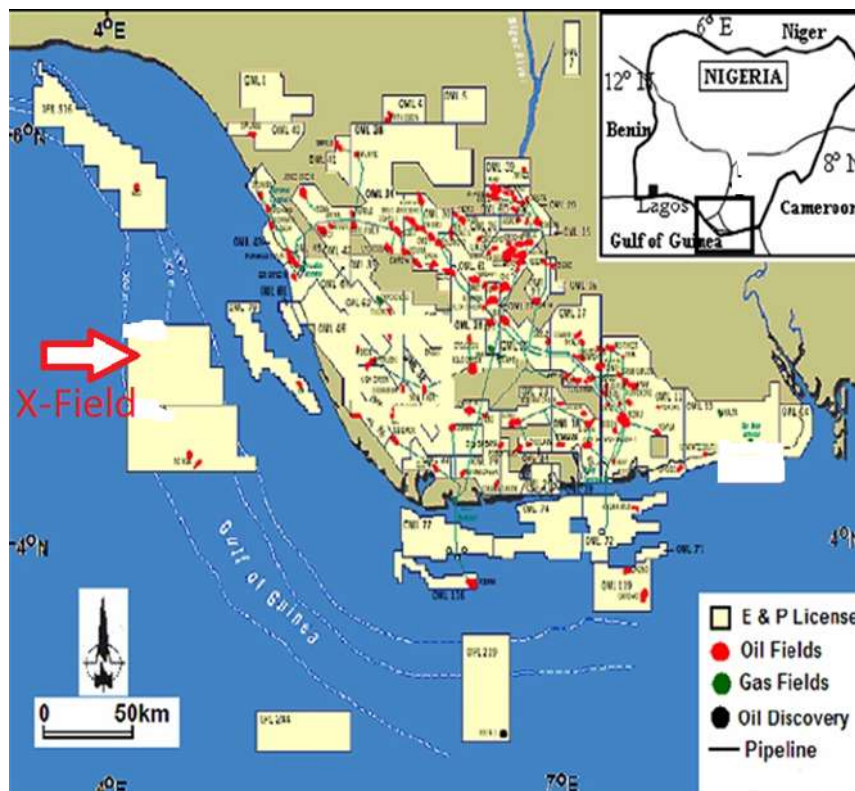


**Figure 1:** Map of the Niger Delta showing the location of the study area (adapted from Nton & Esan, 2010)

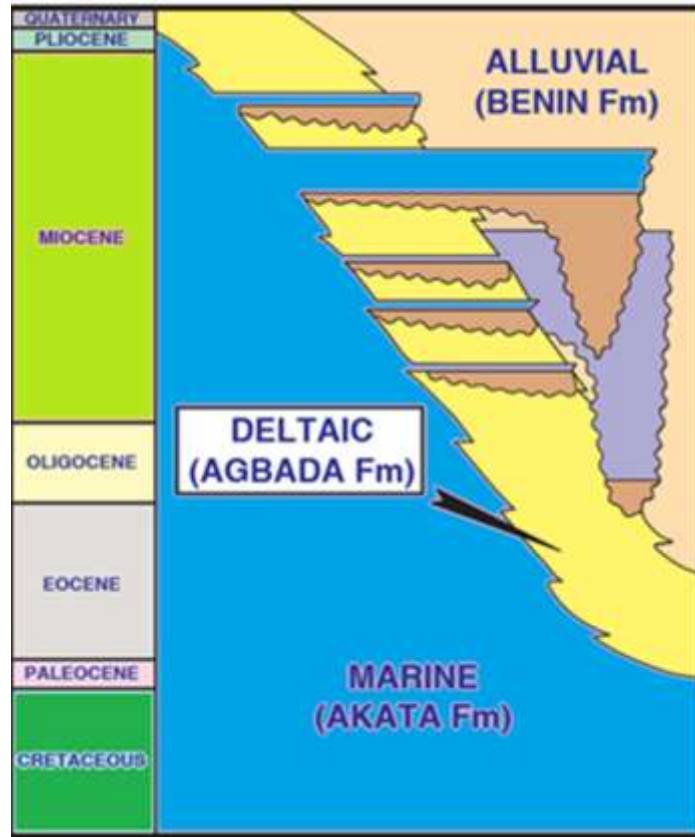


Figure 2: Illustration of the Niger Delta stratigraphy showing the three formations and their geologic ages (adapted from Short & Stauble, 1967).

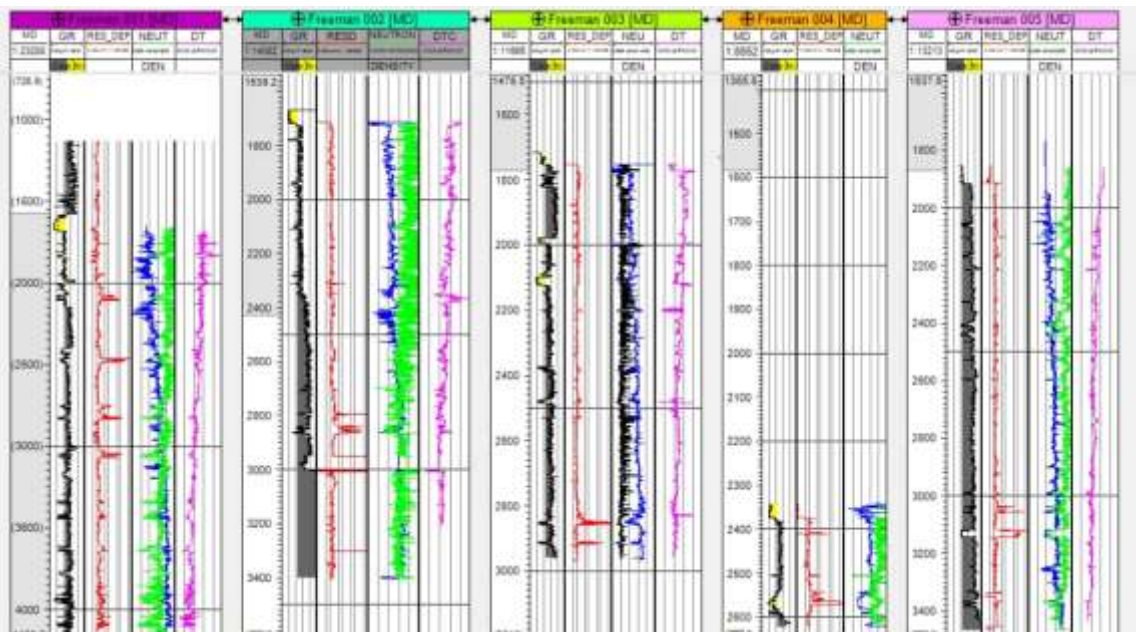


Figure 3: Well log data for wells of the X-field

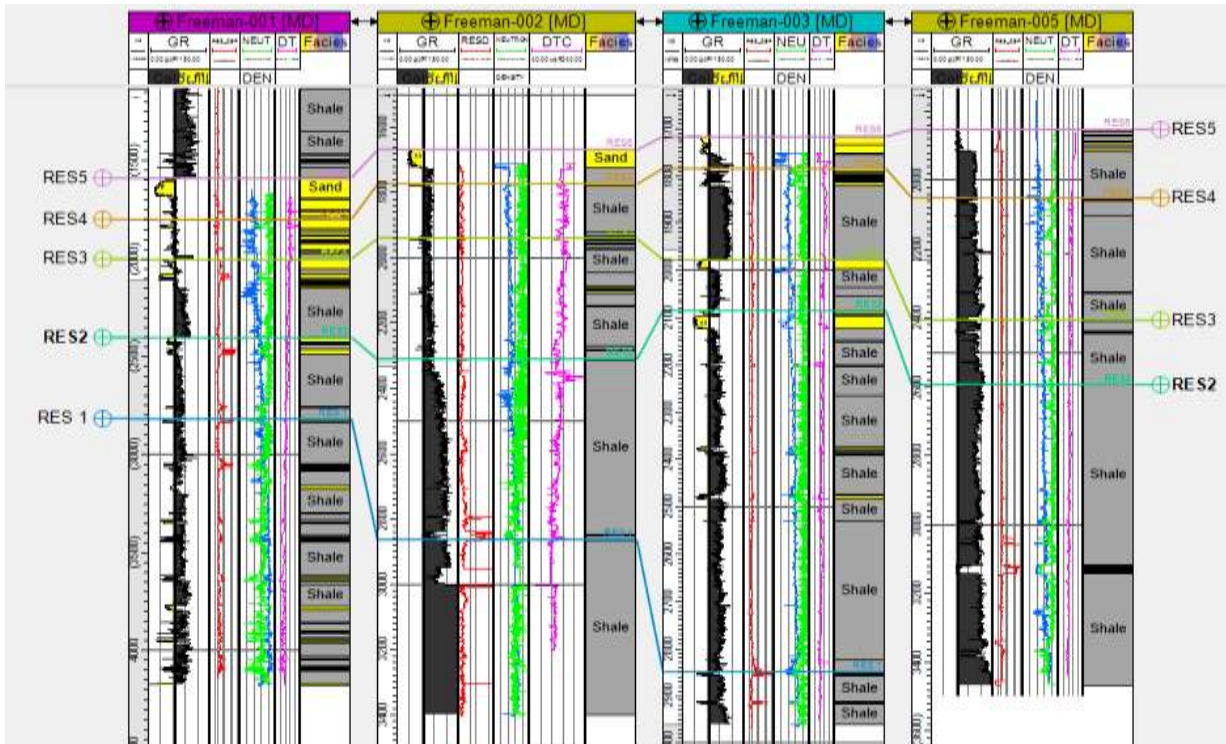


Figure 4: Well log correlation showing the different reservoir tops and genetic units

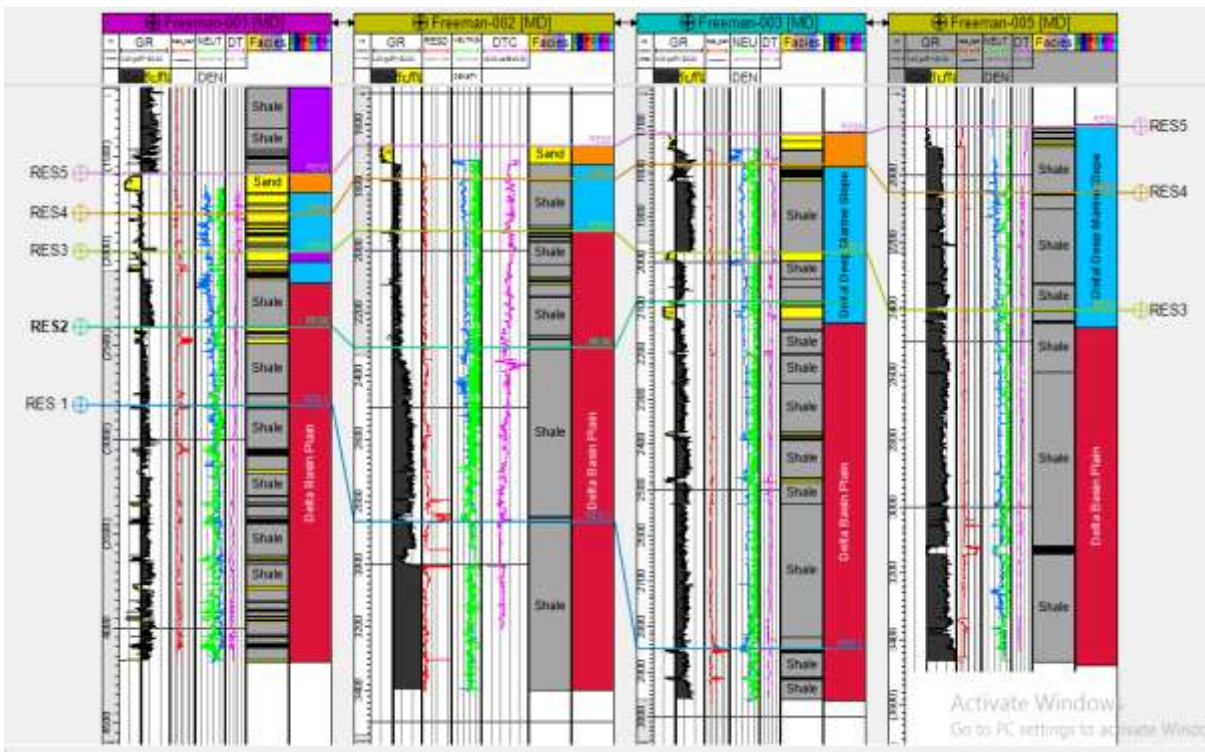


Figure 5: Well log Facies and depositional environment

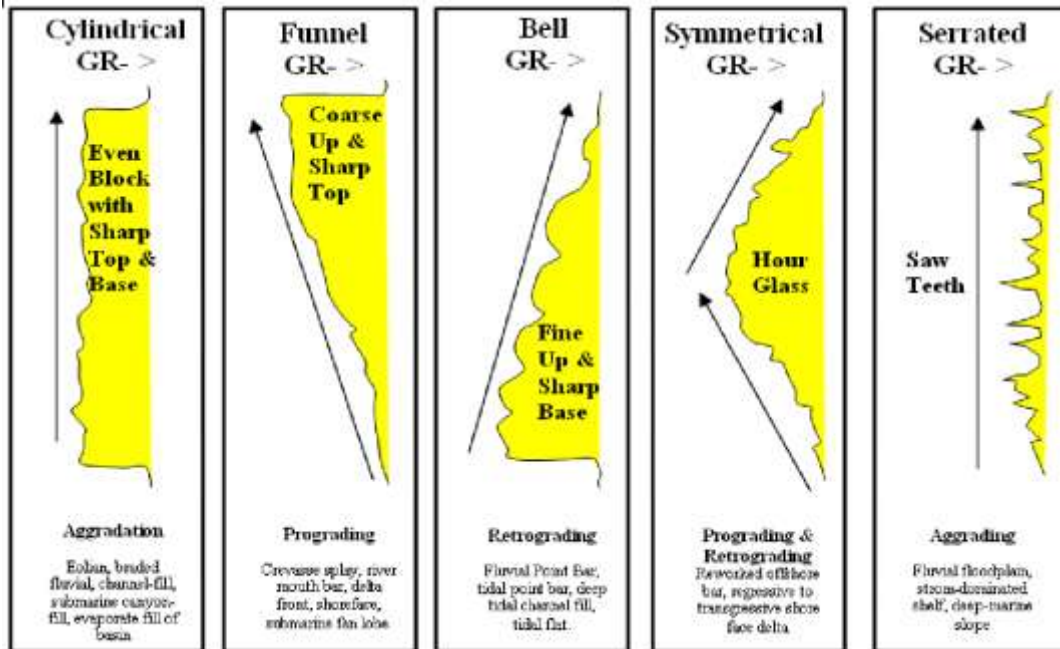


Figure 6: Direct correlation between Facies and log shapes relating to sedimentology (adapted from Cant, 1992)

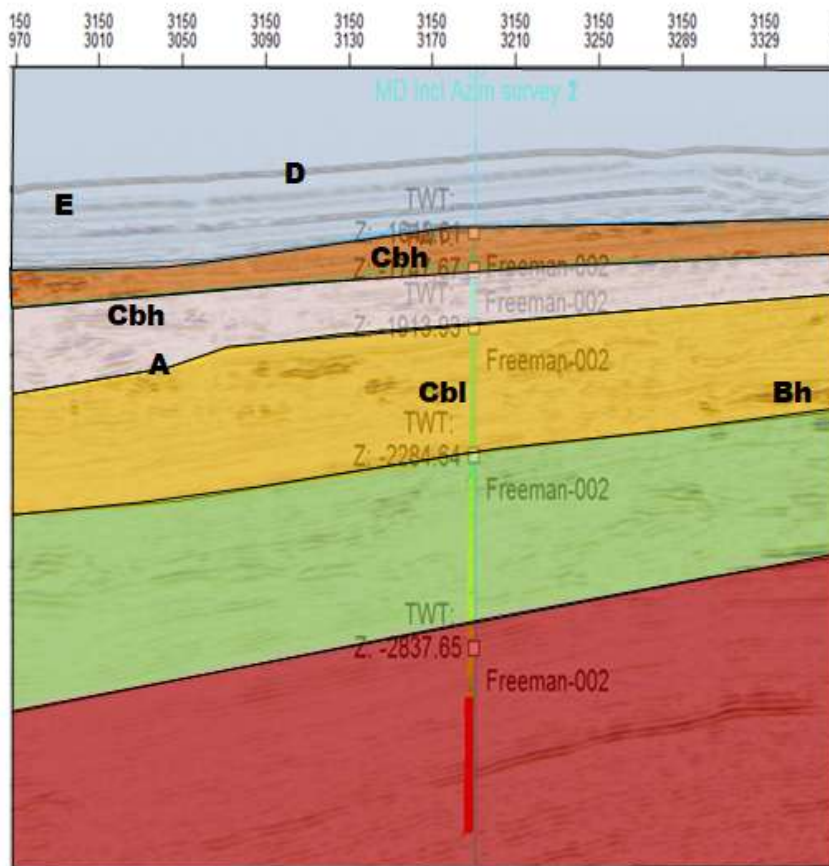


Figure 7: Facies depicted on seismic section

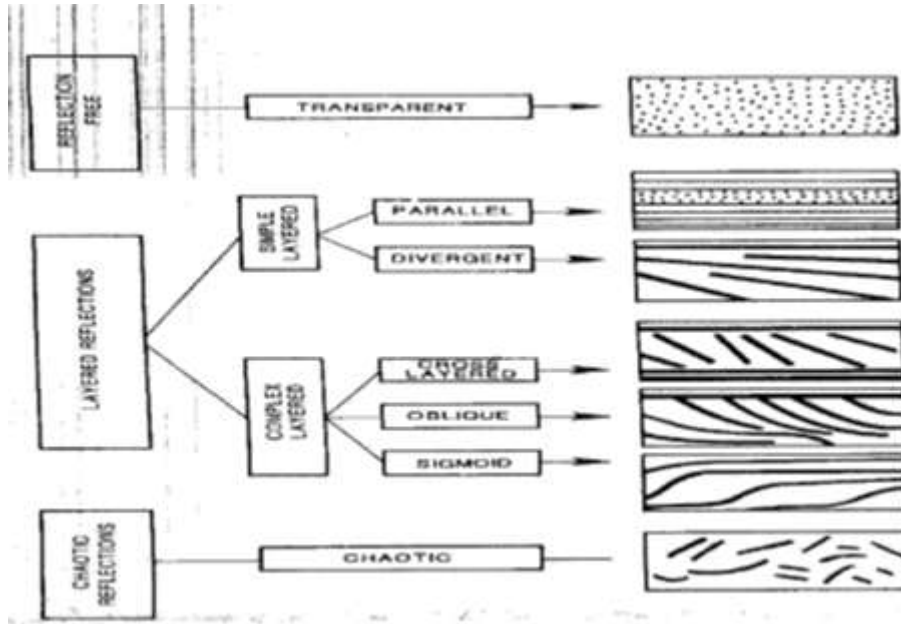


Figure 8: Basic Reflection configuration after Roksandic 2006

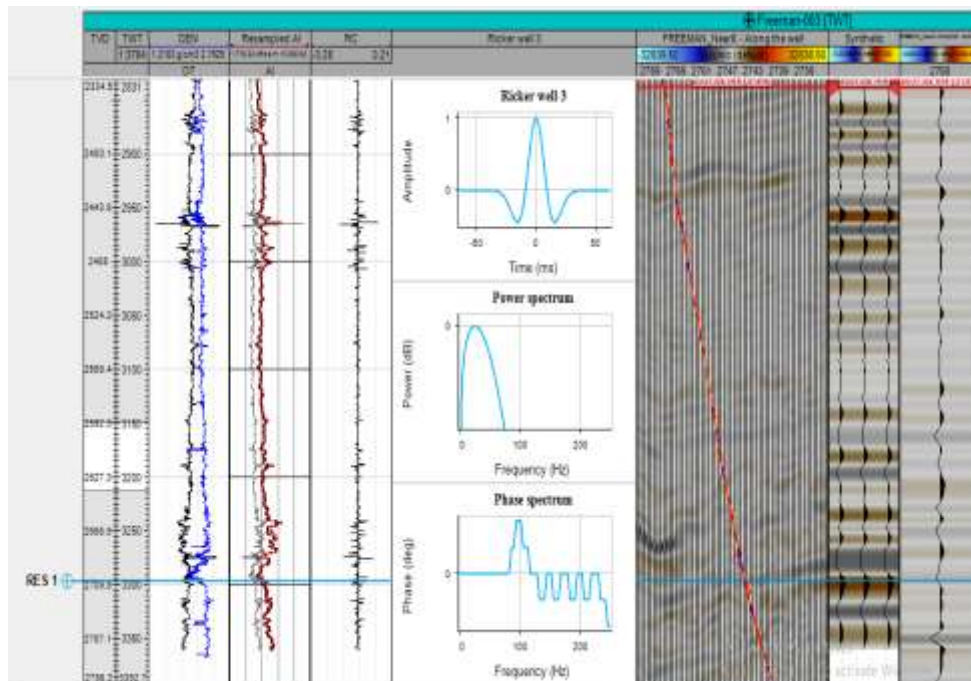


Figure 9: Seismic to well tie using well 03, Ricker 25Hz wavelet, and product of sonic and density log



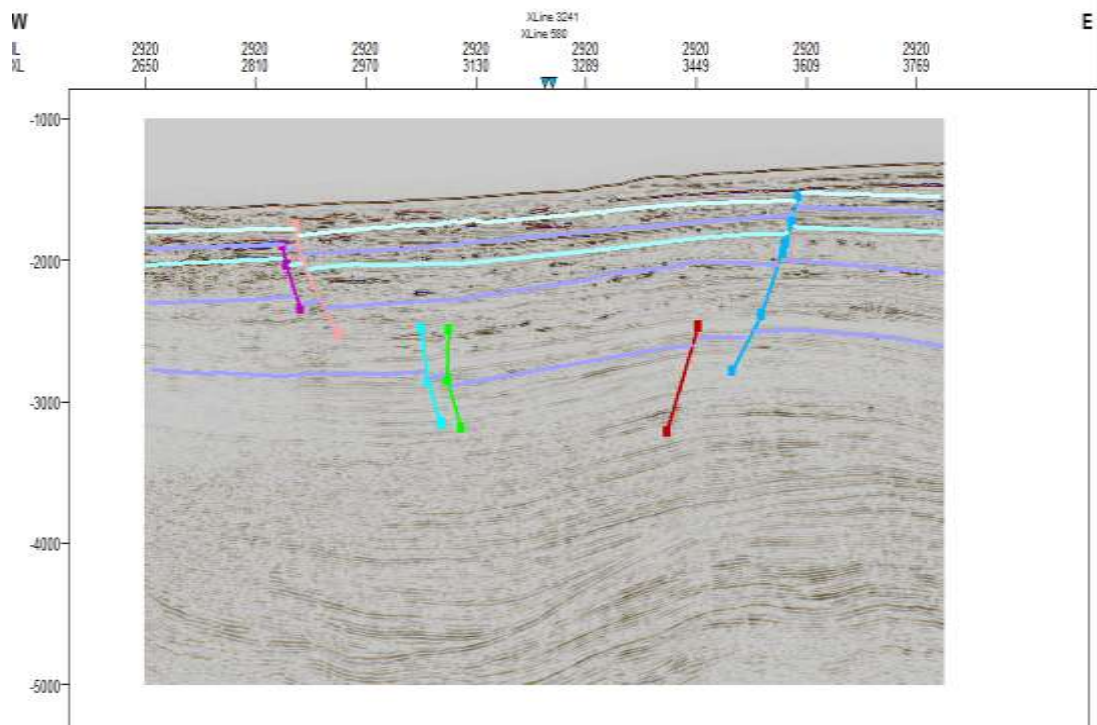


Figure 10: Horizon mapped on seismic line indicating reservoir tops

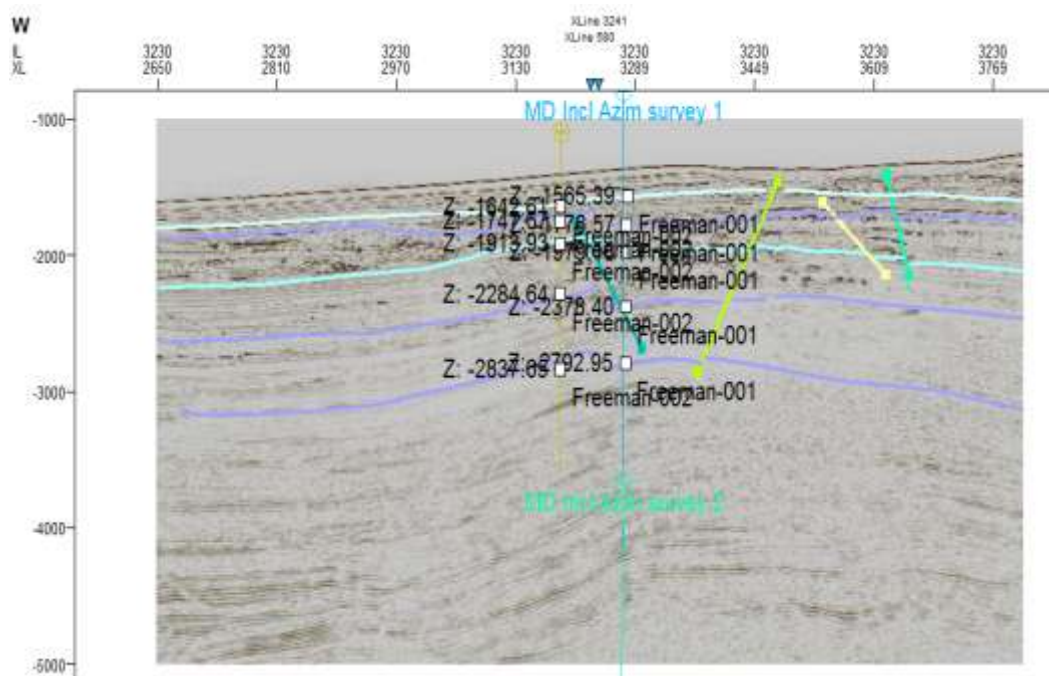


Figure 11: Faults Identified on Seismic Inline 3230

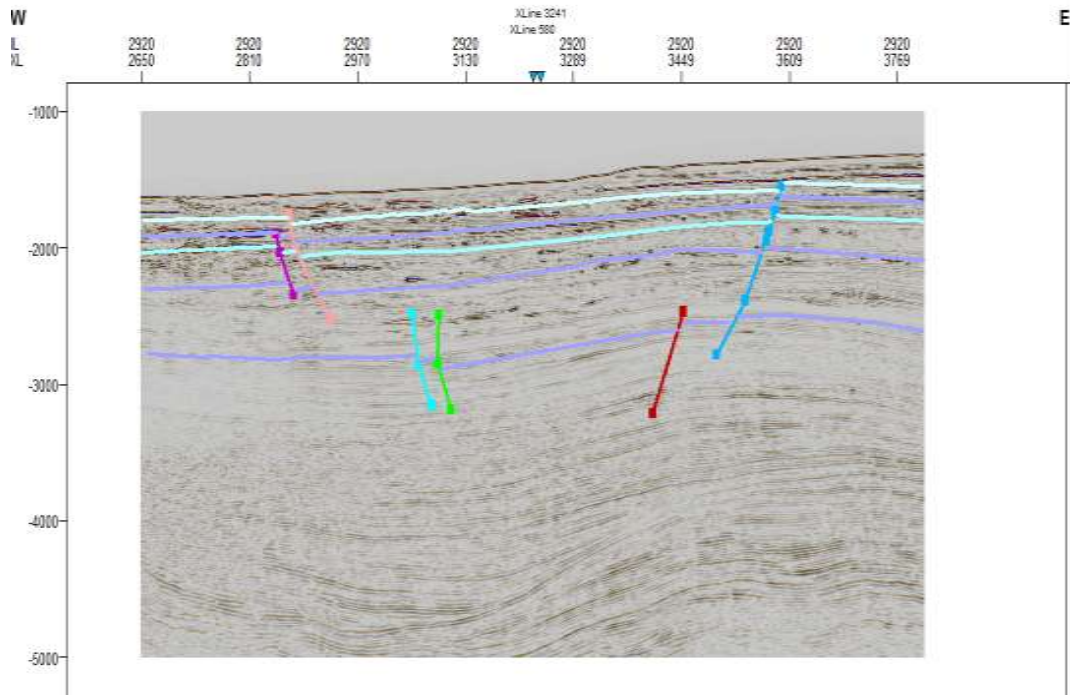


Figure 12: Faults Identified on Seismic Inline 2920

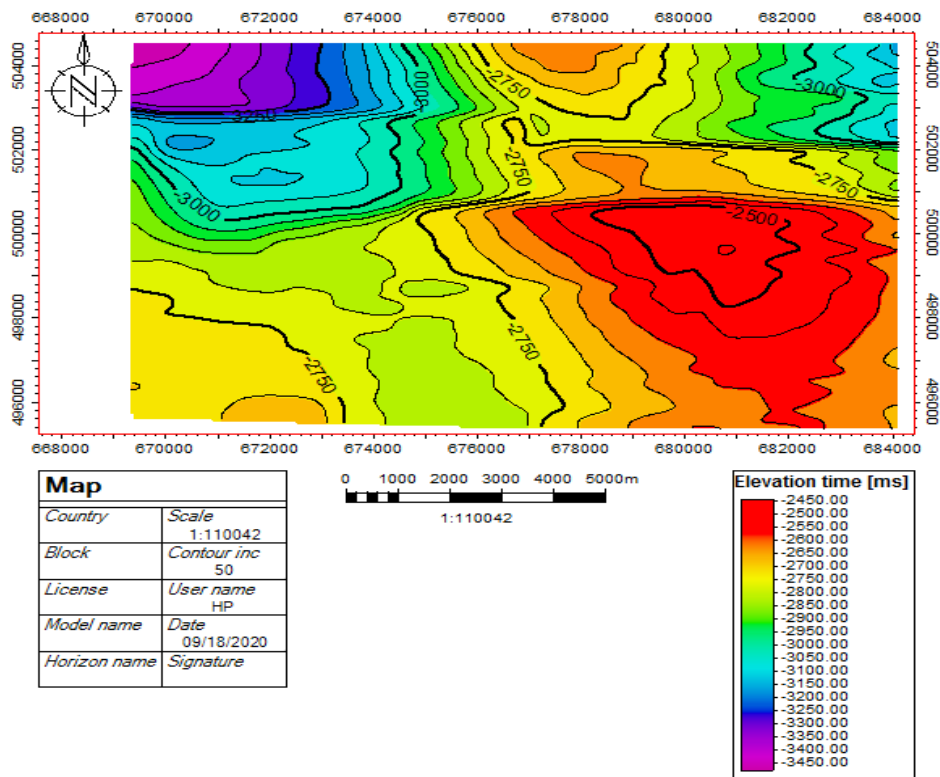


Figure 13a: Time Map for RES 01

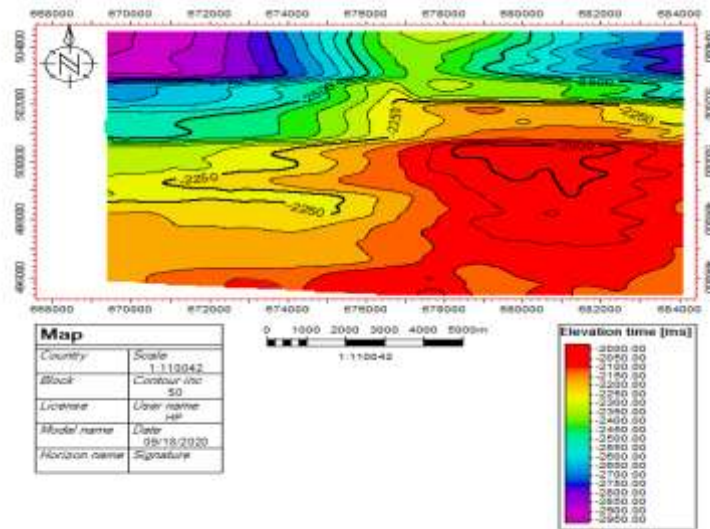


Figure 13b:Time Map for RES 02

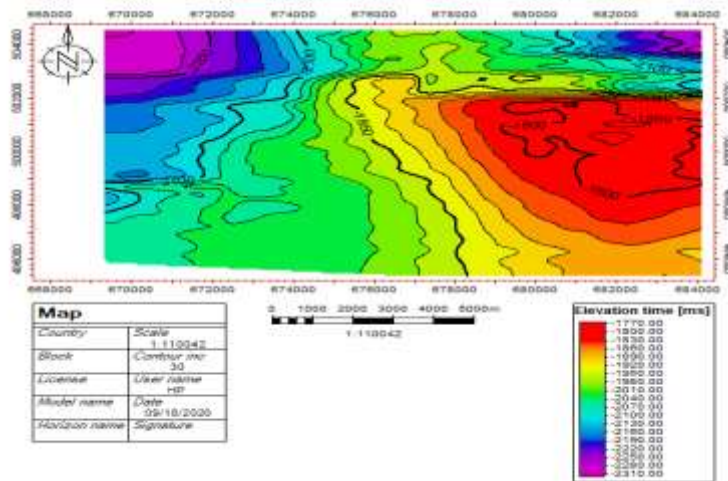


Figure 13c:Time Map for RES03

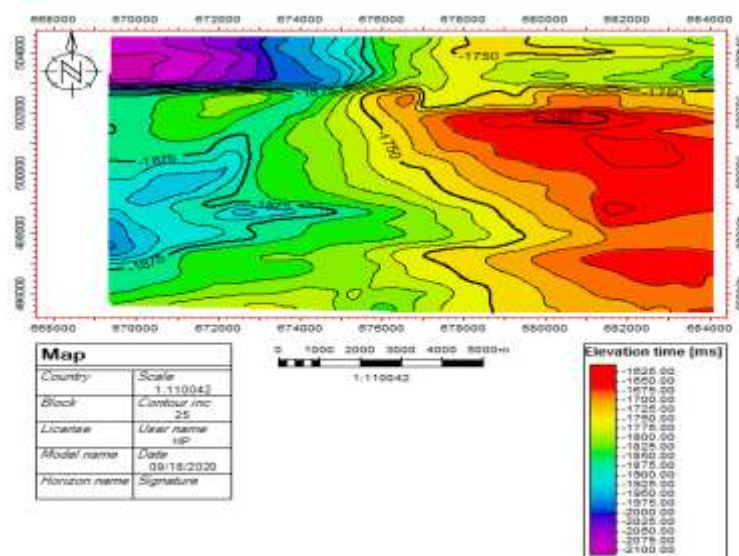


Figure 13d:Time Map for RES 04

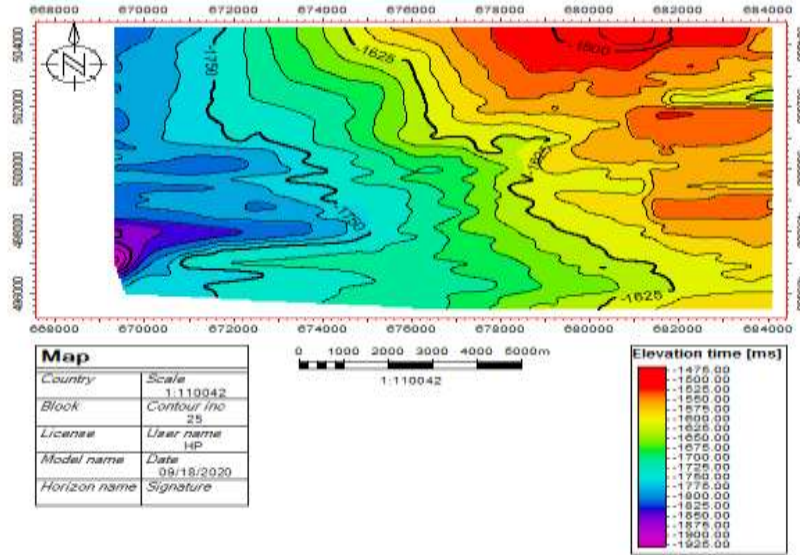


Figure 13e: Time Map for RES 05

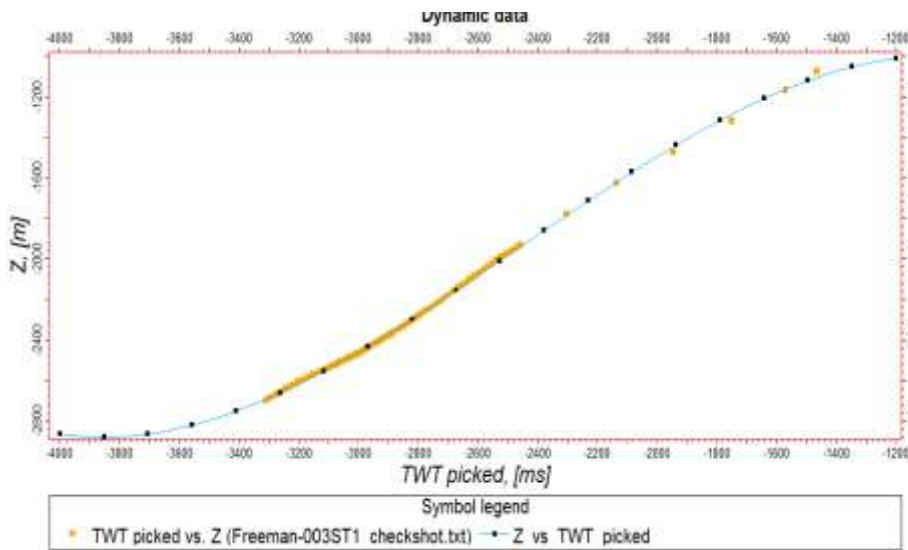


Figure 14: Look-up Function for Depth Conversion

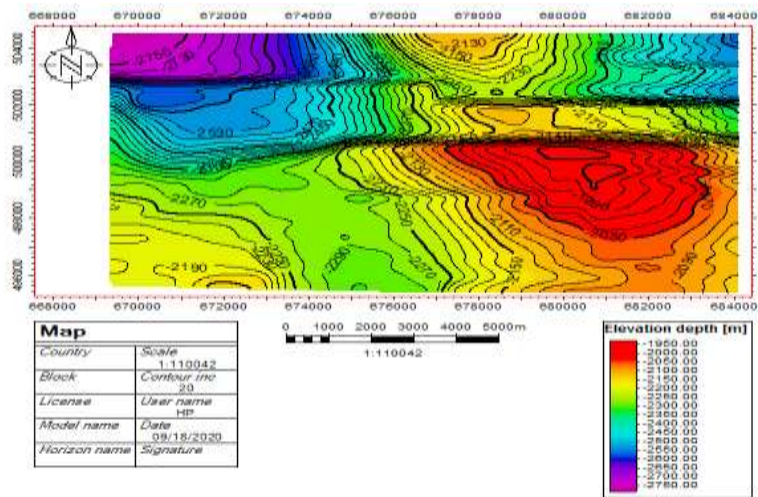


Figure 15a: Depth Map for RES 01

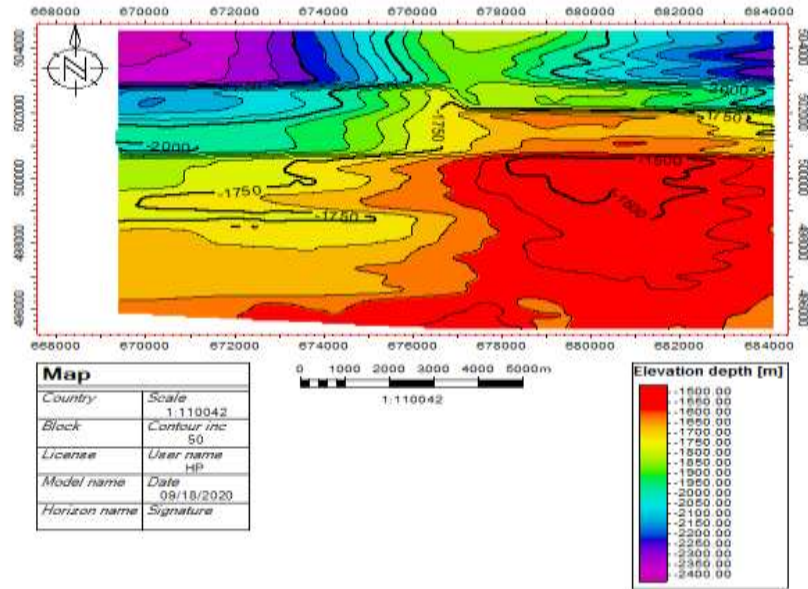


Figure 15b:Depth Map for RES 02

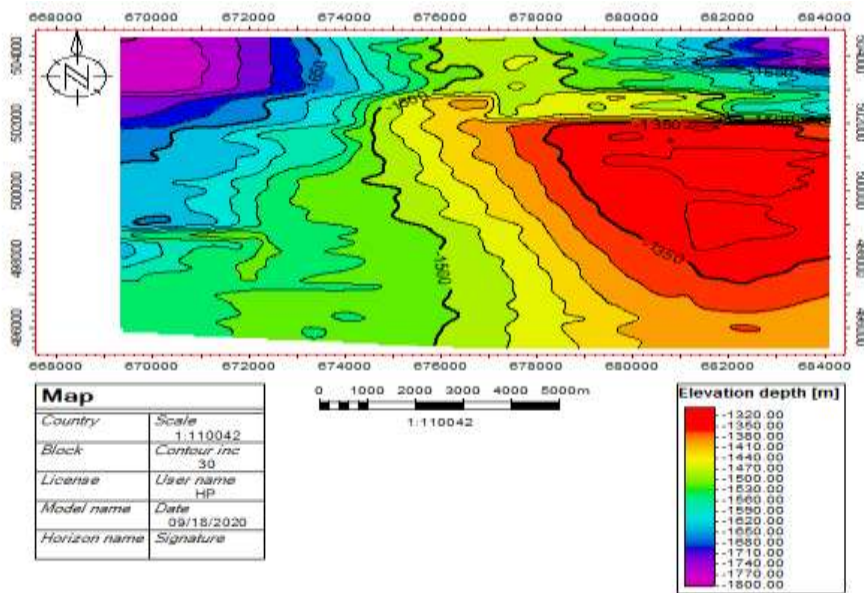


Figure 15c:Depth Map for RES 03

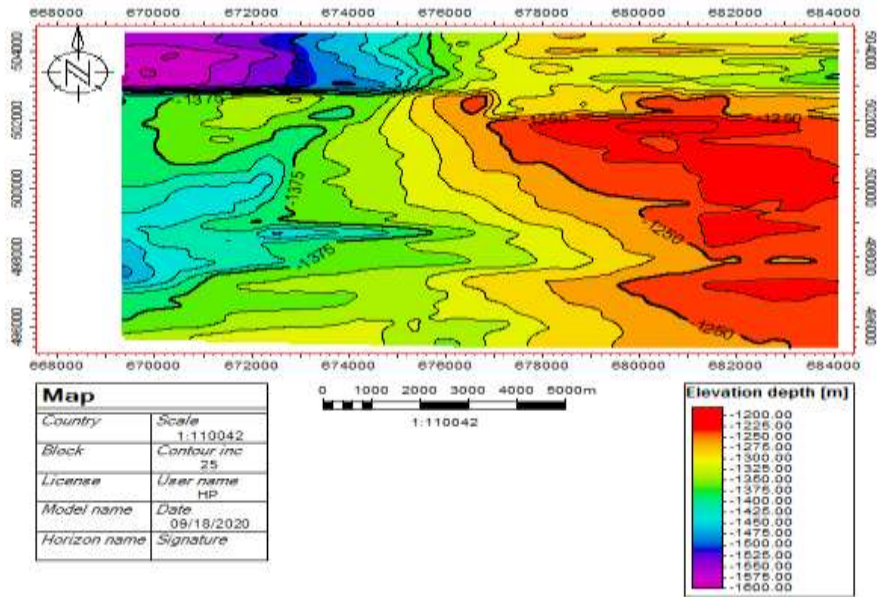


Figure 15d:Depth Map for RES 04

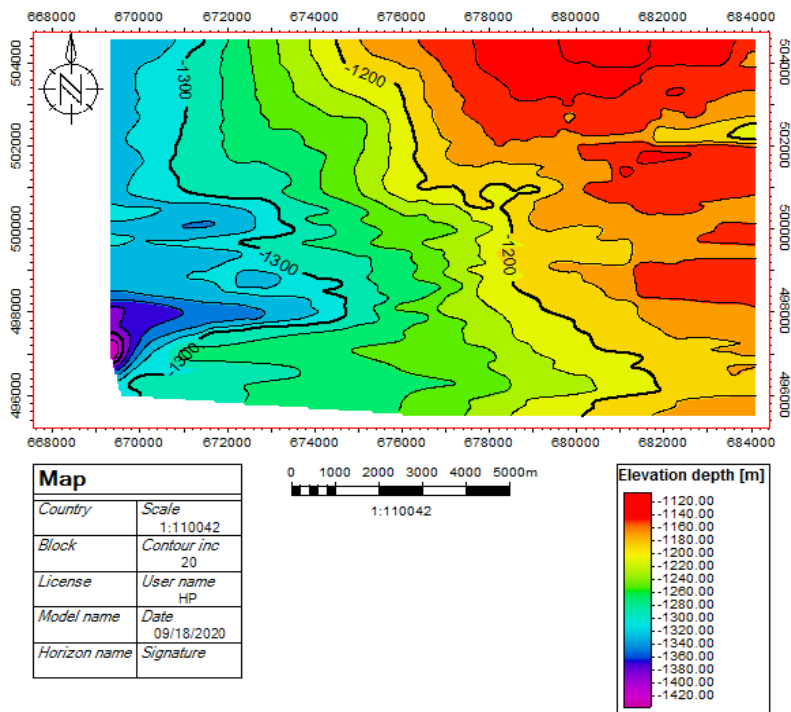


Figure 15e:Depth Map for RES 05

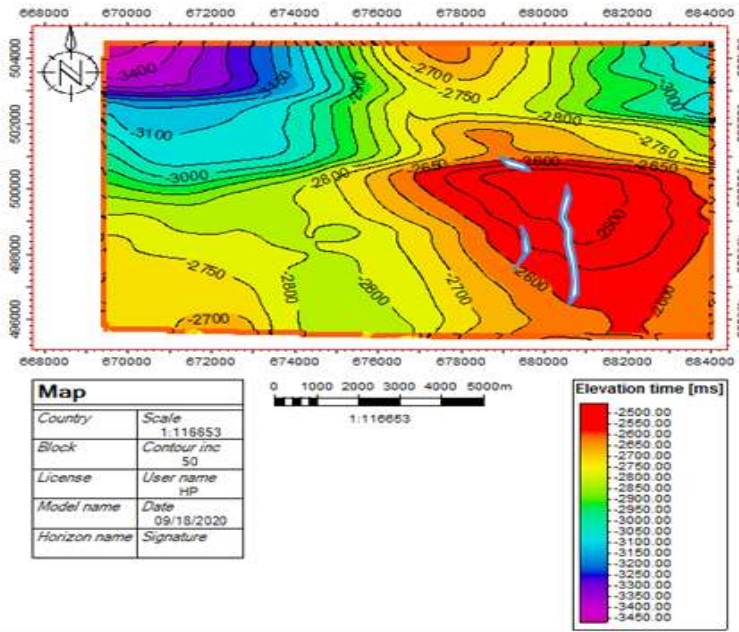


Figure 16a: RES 01 structural map showing 3-way closure fault dependent trap

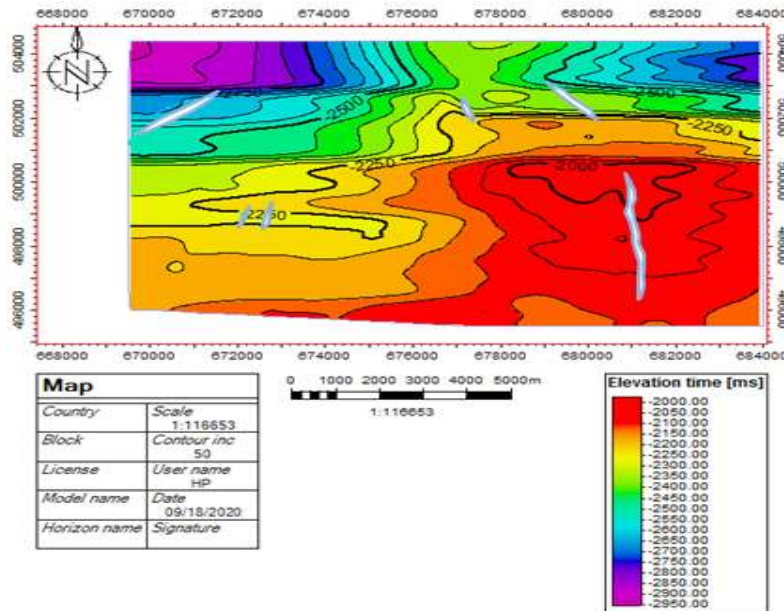


Figure 16b: RES 02 structural map showing 3-way closure fault dependent trap and 2 way closure fault assisted trap

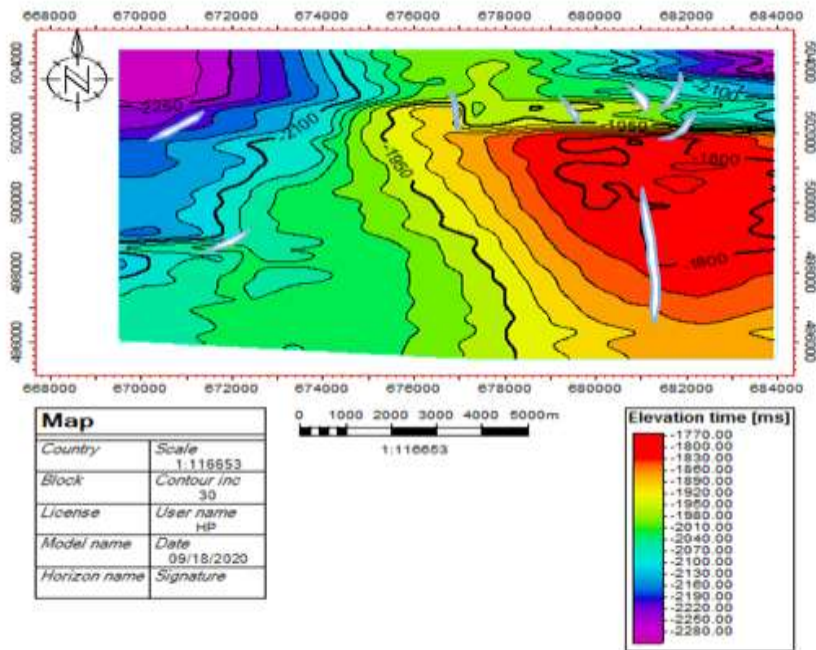


Figure 16c: RES 03 showing 3-way closure fault dependent trap and 2-way closure fault assisted trap

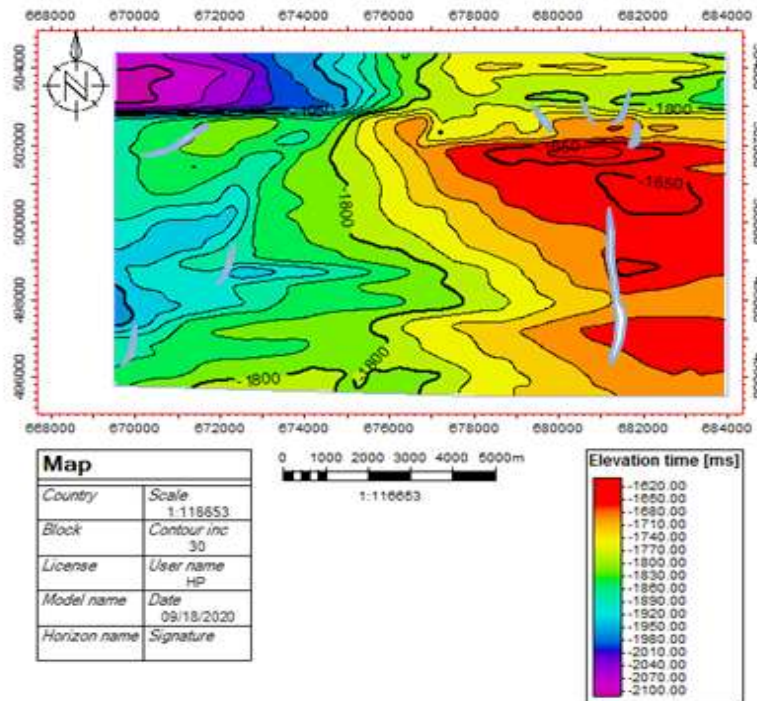


Figure 16d: RES 04 showing 4-way closure anticlinal trap and 3-way closure fault dependent trap



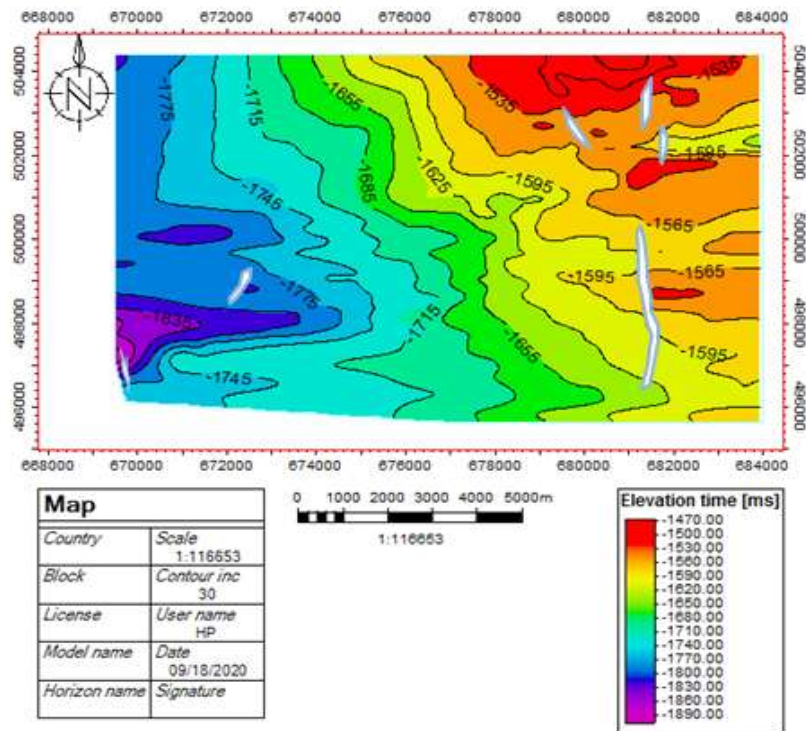


Figure 16e: RES 05 structural map showing 2-way closure anticlinal trap and 3-way closure fault dependent trap

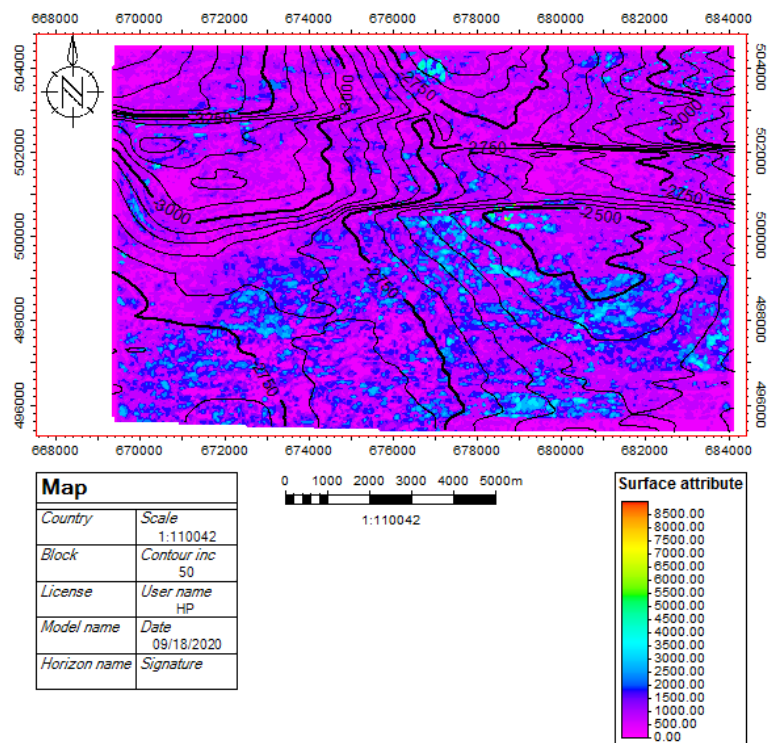


Figure 17a: RES 01 RMS attribute map showing clusters on bright amplitudes in blue

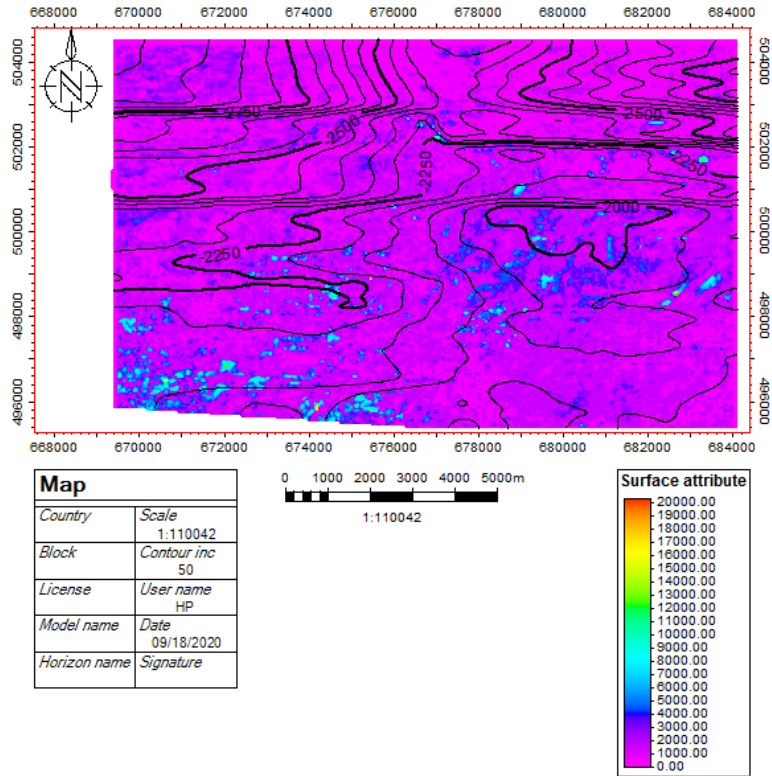


Figure 17b: RES 02 RMS attribute map showing clusters on bright amplitudes in blue

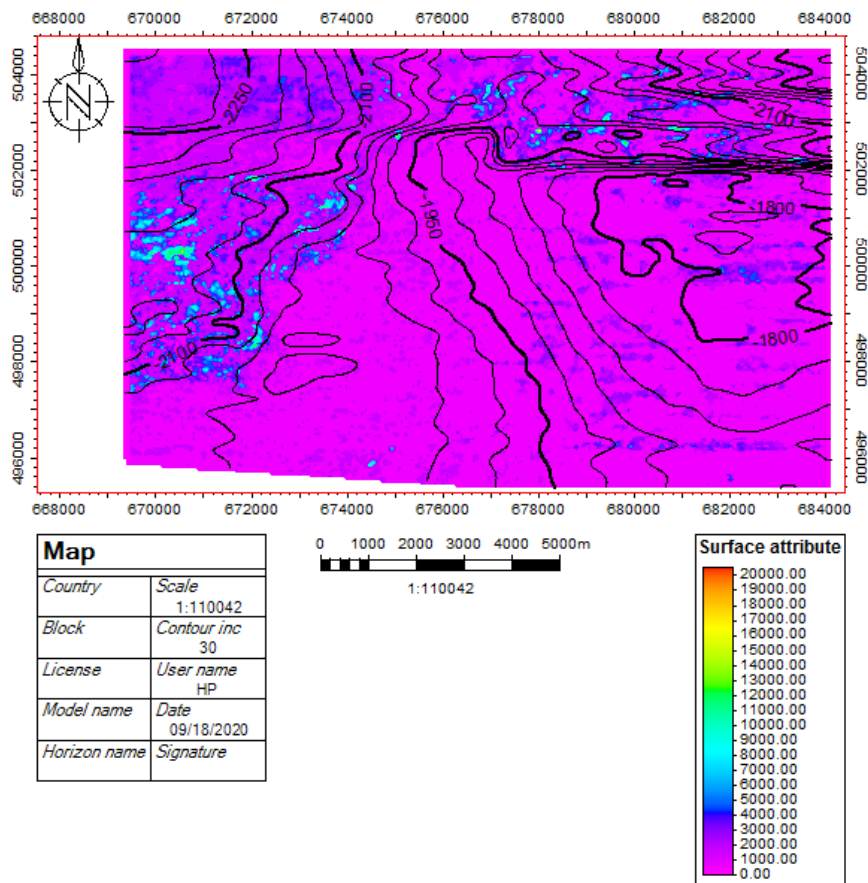


Figure 17c: RES 03 RMS attribute map showing clusters on bright amplitudes in blue

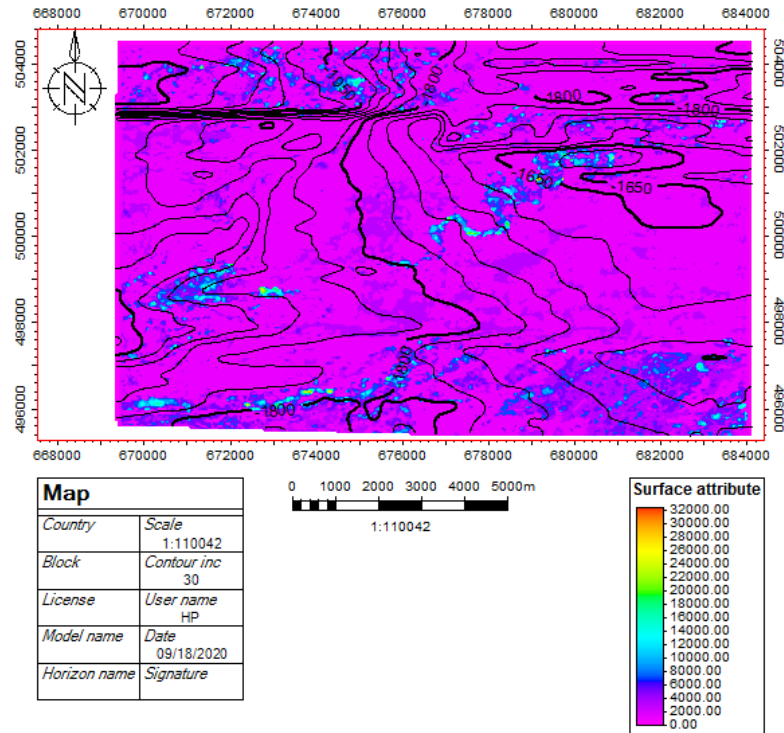


Figure 17d: RES 04 RMS attribute map showing clusters on bright amplitudes in blue

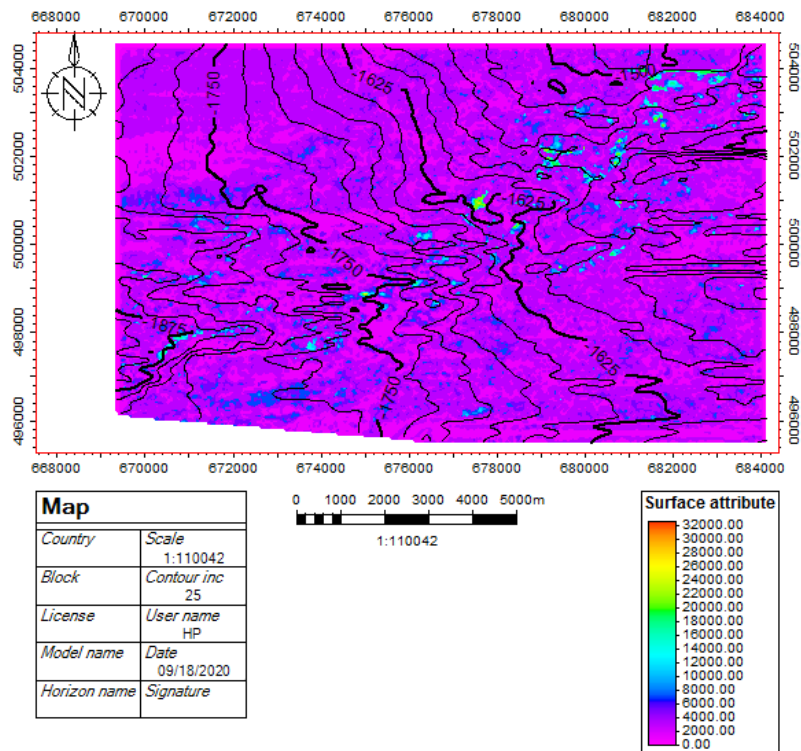


Figure 17e: RES 05 RMS attribute map showing clusters on bright amplitudes in blue

Ikomi, Misan Kelvin, et. al. "Facies Modelling and Reservoir Geometry of the X-Field, Niger Delta Basin, Offshore, Nigeria." *IOSR Journal of Applied Geology and Geophysics (IOSR-JAGG)*, 9(5), (2021): pp 01-19.